Improved Disturbance Observer adhesion control with surface recognition module for Heavy Trains.

Godfrey Makota	Song Wang	Junqi Lu
School of Electrical Engineering	School of Electrical Engineering	School of Electrical Engineering
Southwest Jiaotong University	Southwest Jiaotong University	Southwest Jiaotong University
Chengdu, China	Chengdu, China	Chengdu, China
makotagodfrey@gmail.com	songwang@swjtu.edu.cn	junkin@my.swjtu.edu.cn

***Abstract*—Adhesion control between wheel and rail is a critical factor in the performance, safety and energy efficiency of electric rail traction systems. This paper proposes an adaptive fuzzy based approach for optimal adhesion control in electric heavy duty rail traction. A feedforward fuzzy logic network is trained using simulated adhesion data derived from a dynamic traction model incorporating wheel- rail creep forces and environmental parameters. The proposed controller is integrated into a vector controlled traction drive model in MATLAB/Simulink. Simulation results demonstrates improved adhesion utilization. A six-axle locomotive dynamical model and empirical adhesion characteristic are used to evaluate the methods in single- and multi-axle scenarios. Simulation results demonstrate that the proposed hybrid method substantially improves adhesion utilization, while maintaining robustness across dry, wet, and low-adhesion surfaces. The focus of this paper is on analyzing the adhesion coefficient.**

Keywords: Heavy-duty locomotive, adhesion control, disturbance observer (DOB), fuzzy logic, support vector machine (SVM), adhesion coefficient.

I. INTRODUCTION

A critical performance parameter in electric heavy duty rail traction systems is adhesion control which eventually determine the maximum tractive and braking forces that can be transmitted between the rail and the wheels without excessive slip. Figure 1 shows a six axle heavy duty train .Therefore effective and robust adhesion control strategies are essential to ensure both operational efficiency and safety compliance. Traditional adhesion control techniques typically rely on fixed parameter or simplified wheel-rail models. While effective under steady conditions, their performance deteriorate under nonlinear and time varying scenarios such as wet or contaminated rails, variable axle loads and dynamic braking demands 0.

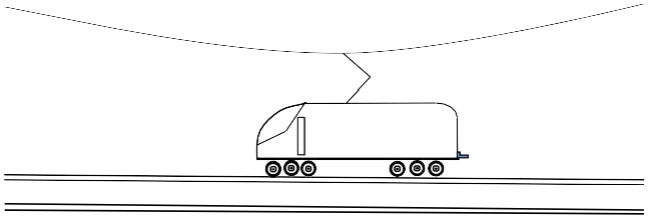

Fig 1. Heavy duty six axle train

Recent advances in traction control and mechatronic systems have enabled the application of intelligent estimation and adaptive control techniques in electric locomotives. However, the highly nonlinear and time-varying nature of wheel–rail contact dynamics, combined with uncertain external disturbances and varying rail surface conditions, makes real time adhesion optimization a challenging problem [2].

In order to address these challenges, this study builds upon the theoretical and experimental framework established. The work systematically analyzes the physical mechanism of wheel–rail adhesion, the locomotive traction system structure, and the adhesion control process. The core contribution lies in the design of an advanced adhesion control architecture that integrates fuzzy rail-surface recognition, support vector machine (SVM) classification, and a disturbance observer–based torque control algorithm [3].

II. LITERATURE REVIEW

Adhesion control is one of the most crucial areas in traction control. Conventional proportional–integral (PI) and threshold-based control algorithms exhibit limitations in dynamic performance and robustness when the adhesion coefficient changes abruptly [4].

The nonlinear and time-varying nature of the wheel–rail contact makes these classical techniques less effective under adverse operating conditions. Recent advances in model-based and intelligent control techniques have sought to address these limitations [5].

A. Wheel–Rail Adhesion Mechanism

The locomotive traction force action model is shown in figure 2 where M is the axle load (23t/25t for heavy-duty

locomotives), g is the gravitational acceleration (usually 9.8 m/s²), T is torque in Nm, r is radius in m, ω_d is angular speed in rad/s, v_t train speed in m/s, F_t traction force in N and F_{ad} adhesion force and normal reaction force N or Wg, Mg. The rotational speed ω_d of the wheelset is always higher than the forward speed v_t of the car body. The slip velocity v_s :

$$v_s = \omega_d \cdot r - v_t \quad (1)$$

The adhesion state can be intuitively expressed by the adhesion coefficient. Due to the complexity of the rail surface condition, the adhesion coefficient is a dispersed random quantity but obeys corresponding statistical laws. Although there is no mathematical expression between creep speed and adhesion coefficient μ, empirical curves of creep speed and adhesion coefficient, i.e., adhesion characteristic curves, can be obtained through a large number of experiments.

$$= - \quad (2)$$

From equation (2), it can be seen that the locomotive traction force F_t is proportional to the adhesion coefficient μ. The adhesion characteristic curve can reflect the variation of traction force i.e. figure 3.

The tractive capability of a locomotive fundamentally depends on the adhesion coefficient between the wheel and the rail. Therefore, it follows that the adhesion coefficient is related to the one with the maximum value of traction force without stopping adhesion. So every adhesion control system tries to operate in this maximum adhesion zone without overshooting by continuously monitoring this peculiar point i.e. the dashed point in figure 3. However the main challenge is that this relationship is a complex one and is a nonlinear function of the slip velocity v_s .

$$\mu = ce^{-av_s} - de^{-bv_s} \quad (3)$$

where a, b, c, and d are parameters that depend on the rail surface condition (dry, wet, or low adhesion).Typical values for a heavy duty train are shown in Table I.

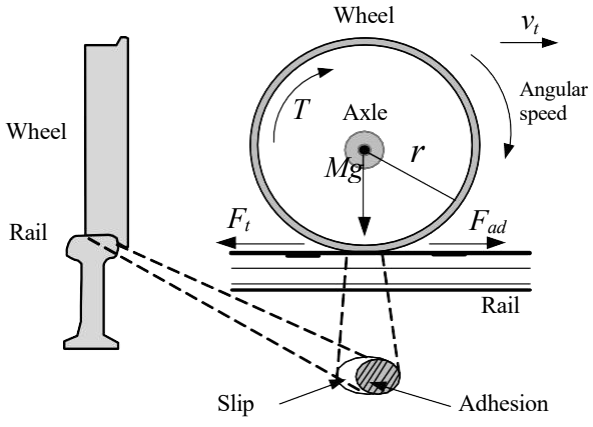

Fig.2 Adhesion mechanism

When the driving torque exceeds the available adhesion force, the wheel begins to slip, leading to energy loss and accelerated wear [6]

Table 1.Rail calculation parameters

Track condition	a	b	c	d	v_s , μ_{max}
Track1(dry)	0.54	1.2	1	1	1.2,0.286
Track2(wet)	0.1876	0.54	0.4	0.4	3.002,0.1487
Track3(low Adhesion)	0.54	1.2	0.4	0.4	1.2099,0.1145

This curve exhibits a rapid rise in adhesion with small increases in slip velocity, reaching a peak value at the critical slip point, and gradually declining beyond it.

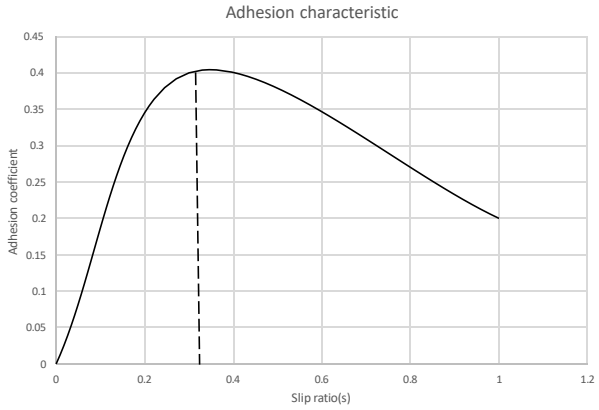

Fig.3 Analysis curve for adhesion characteristics

B. Single-Axle Dynamic Model

In order to analyze the adhesion control process, a single-axle locomotive dynamics model is developed using the derivation formulae, as shown in Fig. 2. The driving torque generated by the traction motor passes through the gearbox to the wheelset, while the adhesion force (F_{ad}) or $F_{adhesion}$ between wheel and rail propels the train forward.

The rotational motion of the wheelset and the translational motion of the vehicle are governed by

$$J_m \cdot \frac{d\omega_m}{dt} = T_m - T_L \quad (4)$$

$$T_L = \frac{F_{adhesion} \cdot r}{R_g} \quad (5)$$

$$R_g = \frac{\omega_m}{\omega_d} \quad (6)$$

$$T = T_m \cdot R_g \quad (7)$$

$$J = J_m \cdot R_g^2 \quad (8)$$

$$J_m \cdot \frac{d\omega_m}{dt} = T_m - \frac{F_{adhesion} \cdot r}{R_g} \quad (9)$$

$$\mu(v_s) = \frac{F_{adhesion}}{W \cdot g} \quad (10)$$

$$\omega_m = \omega_d \cdot R_g \quad (11)$$

$$T_L = \frac{\mu(v_s) \cdot W \cdot g \cdot r}{R_g} \quad (12)$$

$$J \cdot \frac{d}{dt}\omega_d = T - \mu(v_s) \cdot W \cdot g \cdot r \quad (13)$$

$$F_t = T/r \quad (14)$$

$$M_j = J/r^2 \quad (15)$$

$$M_J \cdot \frac{d}{dt} v_a = F_t - \mu(v_s) \cdot W \cdot g \quad (16)$$

the slip ratio can be expressed as: $s = \frac{r\omega - v}{v}$ (17)

A positive slip ratio indicates driving slip, while a negative value corresponds to braking slip. Where J is the equivalent rotational inertia of the wheelset, Tm is the motor electromagnetic torque, R_g is the gear ratio. The final model is shown in figure 4 [7].

C. Vehicle-Controlled Adhesion System Structure

In a vehicle-controlled traction system, all axles receive coordinated torque commands from a single controller, ensuring that torque distribution among multiple traction motors remains balanced.

The control loop typically consists of four subsystems:

1. Driver command unit – provides the reference traction torque.
2. Adhesion controller – estimates adhesion state and computes optimal torque command.
3. Torque control subsystem – executes fast torque adjustments through motor current regulation.
4. Locomotive plant – represents the wheel–rail dynamics and mechanical motion.

This structure forms the basis for designing adaptive and observer-based adhesion control algorithms presented in subsequent sections.

D. Adhesion Characteristics under Different Conditions

Simulation and empirical measurements reveal distinct adhesion parameters under typical environmental conditions. A representative set of parameters, is shown in Table I. The three distinct graphs have the same characteristics increasing then decreasing after a certain critical point shown in figure 8.

E. Model Validation and Simplifications

The model captures the essential nonlinear coupling between wheel rotation and vehicle translation while maintaining simplicity for controller design. The mechanical resistance term F_d is modeled as

$$M \cdot \frac{d}{dt} v_t = \mu(v_s) \cdot W \cdot g - F_d(v_t) \quad (18)$$

$$F_d(v_t) = (a + b \cdot v_t + c \cdot v_t^2) \cdot M \cdot g \quad (19)$$

where a, b,and c represent basic rolling, viscous, and aerodynamic resistance coefficients respectively. The terms a, b, c are resistance calculation coefficients. The resistance coefficients for the heavy-duty electric locomotive in this paper are shown in Table II below:

Table II. Resistance coefficients

Parameters	Value
a	1.67
b	0.0014
c	0.000297

Neglecting higher-order elastic effects of wheel and rail simplifies the model sufficiently for real-time simulation and control testing on a hardware-in-the-loop (HIL) platform [8].

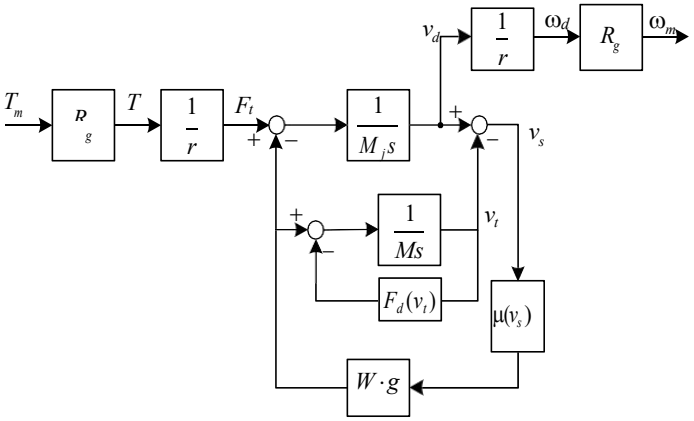

Fig.4 Single axle dynamic model.

III. PROPOSED ADHESION CONTROL STRATEGY AND ALGORITHM DESIGN

A. Overall Control Framework

In order to ensure stable traction performance and optimal adhesion utilization under varying track conditions, a hybrid adhesion control system is proposed. The overall architecture integrates intelligent rail-surface identification, adhesion estimation, and disturbance-observer-based torque control into a unified two-layer framework. This structure forms a closed feedback loop linking the motor torque command, adhesion coefficient, and rail condition classification.

B. Rail-Surface Identification

This paper uses the centroid method for surface identification. Let the membership function of the fuzzy set K surface on the universe U be μ K(u). In the universe U,

$U = \{u_1, u_2, \cdots, u_n\}$ the membership degree of u_i is $K(u_i)$, then the value K surface clear can be calculated by the following equation

$$K = \frac{\sum_{i=1}^{n} u_i K(u_i)}{\sum_{i=1}^{n} K(u_i)} \quad (20)$$

After defuzzifying the fuzzy quantity, its value range is determined by the fuzzy subset obtained from fuzzy inference. The numerical range of these fuzzy subsets may not be consistent with the required numerical range later, requiring scaling transformation, which requires the scaling factor K scale. In this paper, the numerical ranges are consistent, so the scaling factor K scale is taken as 1.

The output after defuzzifying the fuzzy quantity is processed by the data conversion module to obtain the rail surface state identification coefficient K surface. When the output is less than 0.5, the rail surface state identification coefficient K surface value is 0, representing a wet rail surface. When the output is greater than 0.5, the rail surface state identification coefficient K surface value is 1, representing a dry rail surface. The surface identification block diagram is shown in figure 5 below.

$$k_v = \frac{6}{v_{max}} \quad (21)$$

$$k_\mu = \frac{6}{\dot{\mu}_{max}} \quad (22)$$

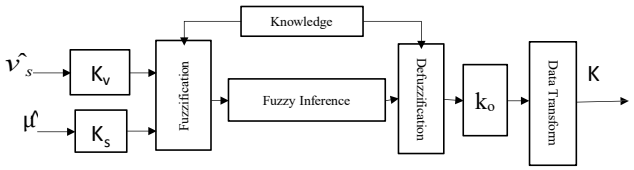

Fig.5 Surface identification block diagram

To enable adaptive control, a two-stage identification mechanism is developed: fuzzy feature extraction followed by SVM classification.

- **1) Input Features**

Measured or estimated variables used for surface recognition include: slip velocity (v_s), slip acceleration $\hat{v}_s$, Torque derivative $\dot{T}_m$ and adhesion coefficient variation rate ($\dot{\hat{\mu}}$).These features are normalized to [0, 1] before processing.

- **2) Fuzzy Feature Extraction**

A fuzzy inference system converts raw signals into linguistic features describing the surface adhesion tendency. Membership functions are defined for Low, Medium, and High adhesion levels based on (v_s) and ($\dot{T}_m$).

Fuzzy rules:

1. *IF* v_s is small *AND* $\dot{T}_m$ is small → Surface = **Dry**
2. *IF* v_s is medium *AND* $\dot{T}_m$ is moderate → Surface = **Wet**
3. *IF* v_s is large *AND* $\dot{T}_m$ is high → Surface = **Low Adhesion**

The fuzzy output vector $f = [f_1, f_2, f_3]$ represents the degree of membership for each condition.

- **3) SVM Classification**

The SVM classifier receives the fuzzy feature vector f and performs final classification using a radial basis function (RBF) kernel:

$$Label = sign\left(\sum_{i=1}^{Ns} \alpha_i \gamma_i K(f, f_i) + b\right) \quad (23)$$

where (Ns) is the number of support vectors, α_i and γ_i are training coefficients and b is the bias term of the SVM decision function and $K(.)$ is the RBF kernel. The output label (Dry, Wet, or Low Adhesion) determines which set of adhesion parameters (a, b, c, d) is applied to the model in Eq. (1) [9, 10, 11].

C. Disturbance Observer–Based Adhesion Estimation

In order to address model uncertainties and unmeasurable disturbances (e.g., rail contamination, load transfer), a disturbance observer is introduced into the torque control loop. The dynamics of the wheelset are given by Eq. (4):

$$\hat{T}_L = \frac{a}{s+a}\left(T_m - J_m \cdot s \cdot \omega_m\right) \frac{1}{R_g} \quad (24)$$

$$\hat{\mu}(v_s) = \frac{\hat{T}_L}{W \cdot g \cdot r} \quad (25)$$

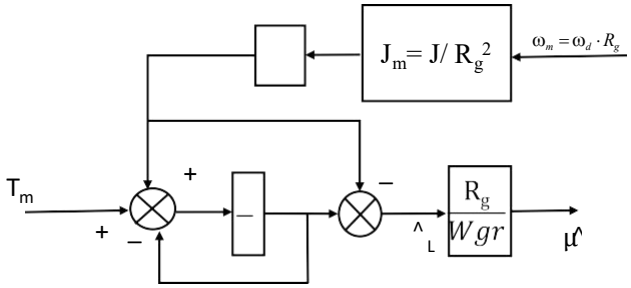

Fig.6 Adhesion estimation module/Disturbance observer.

In equation 24, a is the observer pole of the disturbance observer. Different configurations of the a value obtain different performances. In this paper, a = [100, 10000] can make the observer performance stable and quickly converge. From equations 24 and 25, the observed values $\hat{T}_L$ and $\hat{\mu}$ can be obtained. The observer module is shown in figure 6 [14,15].

D. Adaptive Torque Control Law

The control objective is to maintain operation near the maximum adhesion coefficient (μ_{max}), corresponding to the optimal slip velocity $(v_{s,opt})$ i.e. dashed line in figure 3.The complete block module is shown in figure 7.

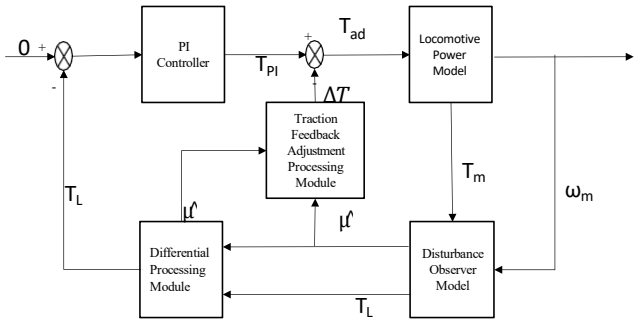

Fig.7. Torque control

$$T_{adhesion} = T_{PI} - \Delta T \tag{26}$$

$$T_{PI} = K_P \cdot \frac{R_g}{W \cdot g \cdot r} \dot{T}_L + K_I \cdot \frac{R_g}{W \cdot g \cdot r} \cdot T_L \tag{27}$$

The gain parameters K_P and K_I are adjusted according to rail condition (wet, dry, low adhesion).

This adaptive adjustment ensures robust performance under both high and low adhesion conditions. The step-by-step execution of the proposed system can be summarized as described. This closed-loop process continuously adapts to track variations and disturbance effects in real time, ensuring stable and efficient adhesion utilization [16, 17,18].

IV. SIMULATION AND RESULTS ANALYSIS

A. Simulation Setup

A single-axle locomotive simulation model was established for comparative simulation analysis. Four scenarios were investigated. The initial traction torque was T_m = 6300 Nm. The simulation environment changed from a dry rail (0-4s) surface to a wet rail surface (4-10s) and then back to a dry rail surface (10-20s).

To verify the effectiveness of the proposed hybrid adhesion control method, a MATLAB/Simulink simulation model was developed based on the theoretical framework discussed in Section III. The model consists of the following subsystems:

- Rail-Surface Identification Module (Fuzzy + SVM)
- Adhesion Observer and Adaptive Torque Controller
- Single-Axle Traction Dynamic Model
- Adhesion Model

Simulation parameters were selected to reflect a typical heavy-duty electric locomotive configuration, as shown in Table III.

Table III. Heavy duty simulation parameters

Parameter	Symbol	Value	Unit
Wheel radius	r	0.45	m
Axle load	N	1.5×10^5	N
Vehicle mass(per axle)	M	1.2×10^4	kg
Rotational inertia	J	75	kg·m²
Rated motor Torque	T_{max}	700	Nm
Simulation step time	T_s	0.001	s

B. Adhesion–Slip-Characteristics

Three rail-surface conditions (dry-track 1, wet-track 2, and low adhesion-track 3) were tested using parameters from Table I. Figure 8 shows the adhesion–slip curves generated from the exponential adhesion model for three rail conditions. The results confirm that peak adhesion decreases and the optimal slip velocity shifts rightward as the rail becomes more slippery

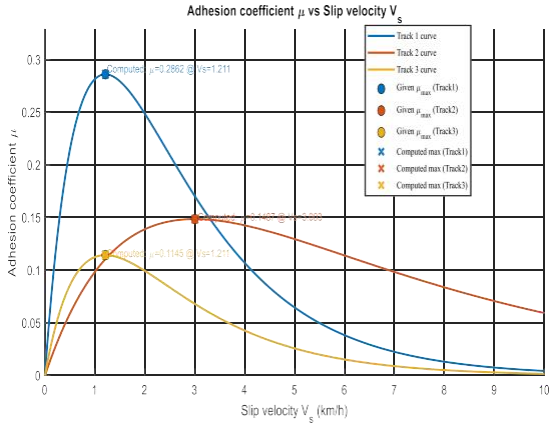

Fig.8. Slip curves under different conditions

C. Slip Velocity and Adhesion Coefficient Tracking

Figure 9 illustrates the corresponding estimated and actual adhesion coefficients, showing accurate tracking by the observer even under abrupt rail-condition changes. It should also be realized at this point that for the adhesion coefficient two value were measured. The bottom graph is for the real value obtained from equation (3) and the other is the estimated obtained from model formulation using static quantities in this case equation (25). Equation (1) is complex and its solution is difficult to get.

Adhesion tracking

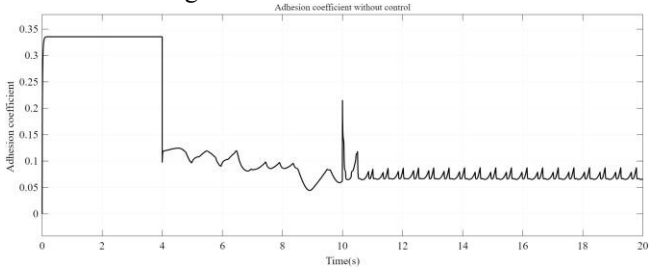

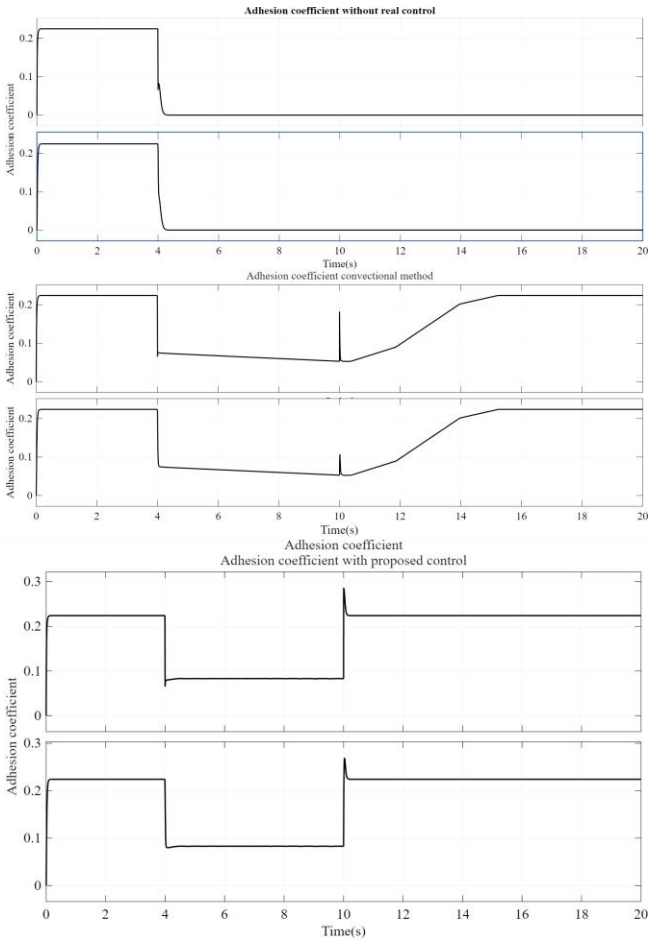

Fig.9 Adhesion Coefficient under various control

D. Vehicle Speed and Adhesion Utilization

The improved adhesion coefficient regulation enhances total traction effort and results in smoother vehicle acceleration. Figure 10 shows vehicle speed trajectories: under low adhesion, the proposed controller achieves about 5 % higher final velocity without excessive slip.

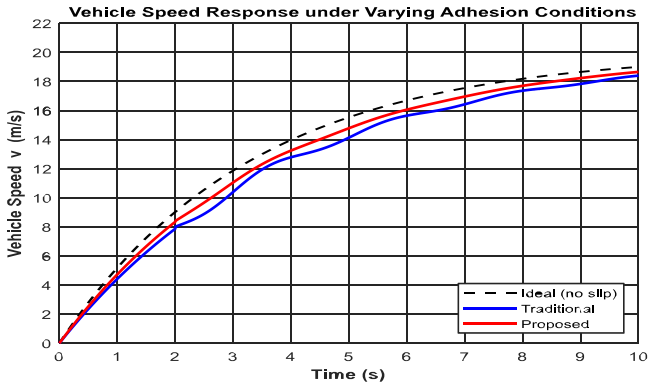

Fig.10 Vehicle speed response under varying adhesion conditions.

Adhesion utilization efficiency is defined as:

$$\eta\mu = \frac{\int_0^T \mu_{eff}(t)dt}{\mu_{\max}.T} \; or \; \frac{\mu_{actual}}{\mu_{\max}} x100\% \qquad (28)$$

Simulations indicate $\eta\mu$ =0.92 for the proposed method versus 0.75 for the traditional control, confirming improved adhesion exploitation.

The designed adhesion control method module based on the disturbance observer ran in the single-axle locomotive simulation. The comparison diagram between the estimated locomotive adhesion utilization coefficient and the actual adhesion utilization coefficient of the locomotive in the simulation is shown in Figure 9. The below graph is the actual rail surface adhesion utilization curve of the locomotive in the simulation, and the above graph is the locomotive adhesion utilization curve estimated by the disturbance observer under different scenarios. The two adhesion utilization curves for each graph are basically consistent, which shows that the locomotive adhesion utilization curve estimated by the disturbance observer is accurate and can be used as a basis for locomotive adhesion control judgment.

E. Summary of Results

Performance metric	Traditional method	Proposed method	improvement
Adhesion utilisation	0.75	0.92	+22%
Speed Fluctuation	±2.5 %	±1.0 %	60% reduction

These results demonstrate that the proposed hybrid controller provides superior adaptability and robustness under diverse rail conditions, ensuring stable traction and improved hauling efficiency.

F. Discussion

The simulation confirms that integrating fuzzy–SVM surface identification with a disturbance observer–based torque controller enables rapid recognition of changing adhesion states. The architecture is scalable to multi-axle locomotives and suitable for real-time implementation on embedded processors or hardware-in-the-loop (HIL) platforms.

V. Conclusion

This paper proposed a fuzzy network-based approach for optimal adhesion control in electric heavy duty rail traction systems. Unlike threshold-based controllers that rely on empirical torque reduction ratios, the proposed algorithm responds proactively by estimating the adhesion limit and compensating for dynamic disturbances. The proposed hybrid adhesion control method demonstrates enhanced dynamic response, improved robustness, and higher adhesion utilization efficiency across diverse rail conditions. These results validate the feasibility of integrating intelligent surface identification with adaptive torque regulation for heavy-duty locomotives.

REFERENCES

[1] Y. Li et al., "Adhesion Control of Heavy Haul Locomotives: A Review," IEEE Transactions on Vehicular Technology, vol. 68, no. 8, pp. 7554–7568, 2019.

[2] Wang, S., Wang, X., Huang, J., Sun, P., & Wang, Q. (2021, August). Adhesion Control of High Speed Train Based on Vehicle-control System. In *2021 IEEE 16th Conference on Industrial Electronics and Applications (ICIEA)* (pp. 142-147). IEEE.

[3] X. Wang and Z. Zhang, "Research on Re-adhesion Control Strategy of Heavy-Haul Locomotives under Complex Conditions," Journal of the China Railway Society, vol. 42, no. 4, pp. 52–59, 2020.

[4] He J, Liu G, Liu J, Zhang C and Cheng X,Identification of a Nonlinear Wheel/Rail Adhesion Model for Heavy-Duty Locomotives [J] , IEEE Access, 2018,6:50424-50432

[5] Zhao Hongwei. HXD1 Electric Locomotive [J]. Electric Drive for Locomotives, 2009, (1): 1-5.

[6] Wang Xiao. Research on Locomotive Adhesion Control Technology [D]. Chengdu: Southwest Jiaotong University, 2012

[7] Djukić, M., Rusov, S., & Mitrović, Z. (2010). A fuzzy model for an increase in locomotive traction force. Transport, 25(1), 36-45

[8] Huang Jingchun and Ren Qiang and Wang Song and Fan Xiaoli, "Electric locomotive adhesion control based on improved disturbance observer," computer simulation, vol. 30, no. 10, pp. 208–212, 2013

[9] Liu W.Y, Han J.G and Lu X.N ,A high speed railway control system based on the fuzzy control method[J] Journal Expert Systems With Applications ,2013.40(15): 6115–6124

[10] R. Palm and K. St0rjohann, "Torque Optimization for a Locomotive using Fuzzy Logic," in *Proceedings of the 1994 ACM symposium on Applied Computing*, 1994, pp. 105–109.

[11] S.-K. Kwon, U.-Y. Huh, H.-I. Kim, and J.-H. Kim, "Re-adhesion control with estimated adhesion force coefficient for wheeled robot using fuzzy logic," in *30th Annual Conference of IEEE Industrial Electronics Society, 2004. IECON 2004*, 2004, pp. 2530-2535 Vol. 3.

[12] Hua C, ban T, ishida M, nakahara T, Influential Factors on Adhesion between Wheel and Rail under Wet Conditions[J] .Jurnal of railway technical institue. 2012.53(04):223-230.

[13] Ishizaka K ,Lewis S.R.and Lewis R,The low adhesion problem due to leaf contamination in the wheel/rail contact:Bonding and low adhesion mechanisms[J] ,International journal of the seince and technologie of friction Wear, 2017, 378-379:183-197,

[14] Smejkal D, Omasta M and Hartl M,An Experimental Investigation of the Adhesion Behavior between Wheel and Rail under Oil, Water and Sanding Conditions[M],Modern Methods of Construction Design. Springer International Publishing, 2014.

[15] Wang, S., Zhang, W., Huang, J., Wang, Q., & Sun, P. (2019). Adhesion control of heavy-duty locomotive based on axle traction control system. IEEE Access, 7, 164614-164622.

[16] Radionov I. A. and Mushenko A.S,The method of estimation of adhesion at"wheel-railway"contact point [C] ,International Siberian Conference on Control and Communications (SIBCON), 2015:1-5.

[17] Sun Jianfang. Research on Adhesion Control Technologyfor Heavy Haul Locomotives [D]. Chengdu: Southwest Jiaotong University, 2013.

[18] Wang, S., Shen, Z., & Huang, J. (2022, May). Adhesion Control of Bogie-Controlled Inner-city Trains. In *2022 IEEE 5th International Electrical and Energy Conference (CIEEC) (pp. 4143-4148).*